



Review of Technologies and Direct Drive Generator Systems for a Grid Connected Marines Current Turbine

R. Gaamouche¹, A. Redouane², A. El Hasnaoui², B. Belhorma³, M. Kchikach², F. Jeffali^{4,5}

¹ Mohammadia School of Engineers, University Mohamed V Rabat, Morocco.

² National Superior School of Mines, Rabat, Morocco.

³ National Centre of Energy, Science and Nuclear Techniques Rabat, Morocco

⁴ Laboratoire de Dynamique et d'Optique des Matériaux, Faculté des Sciences, University Mohamed Premier, Oujda

⁵ High School of Technology, University Mohamed Premier, Oujda, Maroc

Received 17 Oct 2017,

Revised 11 Feb 2018,

Accepted 20 Feb 2018

Keywords

- ✓ Renewable energy ,
- ✓ Marine current prediction,
- ✓ Marine technologies,
- ✓ direct-drive,
- ✓ energy converter systems.

R. Gaamouche

raja.escom@gmail.com

Abstract

The Ocean has provided a new way in the quest for renewable energy. One potential source of energy is the tidal current. The objective of this paper is to carry out a review of systems for the recovery of tidal energy and its conversion into electricity which represents one of the most interesting renewable energy resources precisely Marines Current Turbine MCT. In the first part of this work, a comprehensive description of marine current is performed, in which the physics of tide, the marine current prediction and the tidal Current Kinetic energy extraction models are given. In the second part, a detailed assessment of various state of art MCT systems (horizontal axis, vertical axis, and oscillating Hydroplane Systems), along with their classification and qualitative comparison, is presented. In the last part of this work, an outline of direct-drive electrical generator topologies is sketched in order to identify suitable generator concepts for direct-drive MCT. The comparison of different generator systems in literature is discussed with the criteria based on the energy yield, cost, weight and maintenance problem.

1. Introduction

Today's global energy production is highly dependent on fossil fuel resources such as oil, gas and coal. These resources are limited and their use results in emission of greenhouse gases which has a profound, devastating impact on the environment [1-3]. According to the Kyoto protocol, there is a worldwide agreement to reduce the emission of greenhouse gases [4,5]. To provide a sustainable power production in the future and respecting the Kyoto protocol at the same time, there is a growing demand for energy from renewable sources such as wind, geothermal, solar and ocean [6-8]. At least 30 nations around the world already have renewable energy contributing more than 20% of their national energy supplies [9][10]. Renewable energy application will continue to grow fast in the coming decades as the sustainable development of the human society relies strongly on it [11-13].

As concerning the renewable marine energies, various forms do exist namely tidal energy, wave energy, marine thermal energy, marine osmosis energy, marine biomass energy and offshore wind energy [14,15]. One of the most promising type is the tidal current energy. Indeed, the potential of electric power generated from marine tidal currents is very high [16]. The estimated worldwide tidal current power exploited by existing technologies is 75 GW[17,18]. The identical power harvesting principle similar to wind power generation, the high power density resulting from the seawater property and the high predictability owing to the tidal astronomical characteristics make marine tidal currents particularly attractive and advantageous [19-21].

According to the Electrical Power Research Institute (EPRI) site selection criteria, a viable site for commercial power production normally requires peak currents of 1.5 m/s or greater says Hagerman & Polagye, on 2006[22], although Owen & Bryden have suggested on 2007; it may be as low as 1.0 m/s. For sites that meet this criterion, there is great interest in collecting in-situ data to verify their suitability for tidal power extraction and establish environmental baseline measurements [23].

The MCT is a good alternative to exploit the energy of the tides. This solution involves placing turbines associated electromechanical devices in ocean dumping in areas where the tide develops strong currents [24,25]. This allows producing electric energy locally on the site and sending subsequently to the electric grid in onshore. Nevertheless, it is important to note here that immersion of machines, strong currents and unfavorable weather conditions make MCT systems inaccessible and therefore impossible to maintain for long periods of time [26]. Indeed, the periods of time when it is possible to perform maintenance operations on the machines are short and not very frequent. Maintenance operations are also associated with heavy and specific means and require specialized personnel. Reducing the causes of maintenance and reparation operations is a particularly mattering point to make the power production by marine current turbines economically profitable, and therefore minimize the cost which is higher than other renewable energy sources (the levelized cost (\$/MW) is calculated for wind, solar, tidal (\$1.5 million /Mw, \$4.16 million/Mw, and \$5.45 Million/Mw, respectively) [27-29].

This paper provides a general description of the phenomena that governs the tidal currents and the potential of this resource. Furthermore a not exhaustive description of the principal state of art technological options allowing the harnessing of the tidal currents is presented and the main problems in terms of research and development are also identified. This review will allow us to define the key points to be studied in the future research work.

2. Tidal energy overview

2.1. The physics of tide and current

Tides are generated by the rotation of Earth and its surrounding ocean envelope which is shaped by the gravitational fields of Moon and Sun [22,30]. The Moon's gravitation creates tidal "attractive forces" that create two "bulges" in Earth's ocean envelope: one bulge on the side of Earth facing Moon, and the other bulge on the opposite side of Earth. Rotation of Earth and these "bulges" result in two tides (high water to low water sequence) per day, called semi-diurnal tides, two of them depict the dominant tidal pattern in most of the world's oceans [11,31]. In fact, the combined lunar-solar tidal bulge is predominantly lunar with a solar related adjustment that affects the height of the tide and the direction of the tidal bulge according to the phases of Moon. During the times of new and full Moon, when Earth, Moon, and Sun lie approximately on the same line resultant tides are called spring tides (Figure 1.a). Meantime between spring tides, when Moon is at first and third quarters, Sun's tidal forces act at right angles to Moon's tidal forces, creating lower high tides and higher low tides. The resulting tides are called neap tides (Figure 1.a).

In summary, every full Moon and every new Moon, circa periodically, tidal amplitudes go through a maximum. And each first and last quarter, they go through a minimum (Figure 1.b) [11,32].

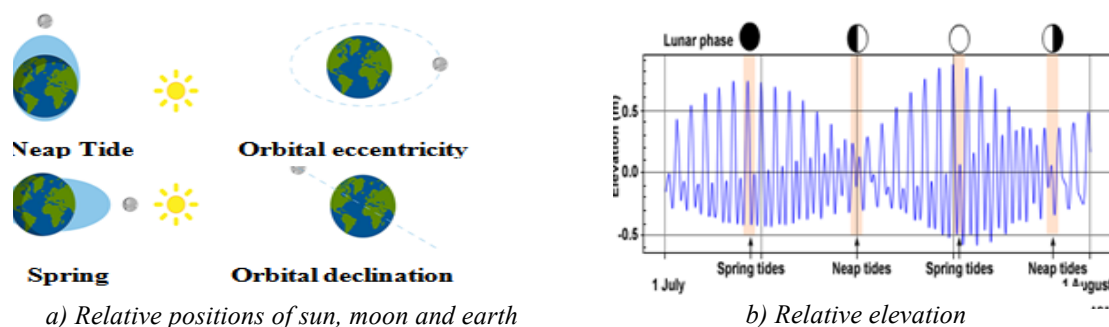


Figure 1 : Spring and neap tides[32].

Thus, the tide height at a time instant t can be expressed by the following formula [33] [34] :

$$h(t) = H_0 + \sum_{i=1}^n [A_i \cos (\omega_i t - \varphi_i)] \quad (1)$$

Where:

H_0 is the sea mean height and A_i , ω_i and φ_i are the amplitude, the angular speed and the phase angle of individual harmonic elements respectively. Amplitude and phase angle, known as harmonic constants, are unique for every location, while the angular speed (in degrees per solar hour) for each harmonic element is calculated by astronomical knowledge of the motion of Earth Sun and Moon, and thus constant for all the sites. So, all what have been left to be calculated is the amplitude and the phase angle. In Table 1 a list of these tide model components is given [35].

Table 1 : Principal tidal harmonic elements.

Harmonic element	ω_i	A_i	φ_i
M_2	$2T-2s+2h=28.984$ degrees/solar hour	not know	not know
N_2	$2T-3s+2h+p=28.439$ degrees/solar hour	"	"
S_2	$2T = 30.000$ degrees/solar hour	"	"
K_1	$T+h = 15.041$ degrees/solar hour	"	"
O_1	$T-2s+h = 13.943$ degrees/solar hour	"	"
M_4	$2xM_2=57.968$ degrees/solar hour	"	"
M_6	$3xM_2=86.952$ degrees/solar hour	"	"

Where:

T the rotational speed of the Earth around its axis, with respect to the Sun, 15 degrees/hour,

h the rotational speed of the Earth around the Sun, .04106864 degrees/hour,

s the rotational speed of the Moon around the Earth, .54901653 degrees/hour,

p the precession of the Moon's perigee, .00464183 degrees/hour,

N the precession of the plane of the Moon's orbit, -.00220641 degrees/hour.

Equation (1) then is simplified for a predicted tide to equation (2) shown below:

$$H(t) = H_0 + A_{M_2} \cos(\omega_{M_2}t + \varphi_{M_2}) + A_{N_2} \cos(\omega_{N_2}t + \varphi_{N_2}) + A_{S_2} \cos(\omega_{S_2}t + \varphi_{S_2}) + A_{K_1} \cos(\omega_{K_1}t + \varphi_{K_1}) + A_{O_1} \cos(\omega_{O_1}t + \varphi_{O_1}) + A_{M_4} \cos(\omega_{M_4}t + \varphi_{M_4}) + A_{M_6} \cos(\omega_{M_6}t + \varphi_{M_6}) \quad (2)$$

Tide coefficients above characterize the tide's strength. Figure 2 presents the tide's high and low successive (marling) and tide's coefficient variations (2 tides per day) for the port of Casablanca in March 2016. It is worth noting here that:

- ✓ When the marling and the coefficient of tide go through a maximum, the tide is known as spring tide. It corresponds to the phase of the new Moon and full Moon.
- ✓ When the marling and the coefficient of tide go through a minimum, the tide is called neap.

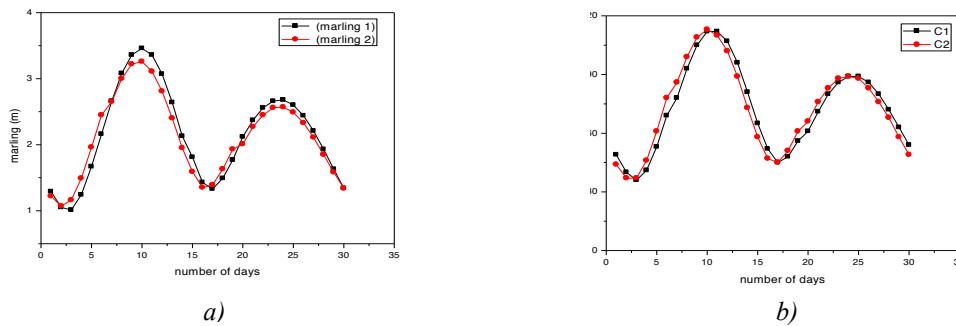


Figure 2 : a) Marling variation in March 2016 at the port of Casablanca, b) Tide coefficient variation in March 2016 at the port of Casablanca

2.2. Marine current prediction

Tidal Current is the horizontal movement of the water caused by gravitational interactions between Sun, Moon, and Earth. It is part of the same general movement of the sea that manifest in vertical rise and fall called tide [34]. Tidal current is the horizontal component of this particulate motion, while tide denominates the vertical component. The observed tide and tidal current can be considered the result of the combination of several tidal waves, each of which may vary from nearly pure progressive to nearly pure standing and with differing periods, heights, phase angels, and directions [35].

To predict and calculate the expected annual energy captured from a tidal current turbine, it is necessary to determine the marine current. In fact, there are two ways to determine the speed of tidal currents [11,24] :

- Either by direct measurement, using conventional devices such as helical current meters and Doppler profilers or by a practical model proposed by the SHOM (French Navy Hydrographic and Oceanographic Service) [36].
- Either by modeling, there are several methods to model the marine current such as Harmonic Analysis Method (HAM), Double Cosine Method, Tidesim, Tide 2D [11,38].

In this paper, an overview of the most useful techniques for determining tidal current will be discussed: HAM, Double Cosine Method and the practical model of SHOM.

a. Harmonic Analysis Method

As already mentioned, the tidal height can be derived from the equation (1), so it is possible to predict the variation in water height from astronomical influences at a particular location to a good degree of quality via the use of harmonic analysis of a tidal record of at least 30 days. The tidal speed can then be calculated as follows [11,37,38]:

$$V(t) = \sqrt{2g(H_1(t) - H_2(t))} \quad (3)$$

Where:

g is the gravitational constant (9.8 N/kg),

H_1 is the water height of first site (m),

H_2 is the water height of second site (m).

The obtained flow velocity is then corrected for channel losses by introducing a channel loss coefficient, K_L as follows:

$$V(t) = K_L \sqrt{2g(H_1(t) - H_2(t))} \quad (4)$$

The value of K_L is calculated using an idealized channel model based on Manning's equations for open channel flow rate:

$$V = \frac{k R^{\frac{2}{3}} S^{\frac{1}{2}}}{n} \quad (5)$$

$$R = \frac{\omega d}{\omega + 2d} \quad (6)$$

$$S = \frac{d_1 - d_2}{l} \quad (7)$$

$$K_L = \frac{k R^{\frac{2}{3}} S^{\frac{1}{2}}}{n \sqrt{2g(H_1(t) - H_2(t))}} \quad (8)$$

This model strongly depends on the harmonic elements, as well as on the hypothesis for the channel. The main advantage of this method is that it makes it possible to calculate the speed step by step [39].

b. Double Cosine

The tidal cycle has been approximated by a double sinusoid, one with a period of 12.4 hours representing the diurnal period T_0 , and the other a period of 353 hours representing the spring neap period T_1 . The following equation, as given by Fraenkel [40], provides a conceivable model for the prediction of the tidal current [40] [41,42]:

$$V = [K_0 + K_1 \cos(\frac{2\pi t}{T_1})] \cos(\frac{2\pi t}{T_0}) \quad (9)$$

Where K_0 , and K_1 are constants derived from the mean spring peak and the ratio between the mean spring peak and the mean neap peak current velocities'.

This method, which accounts for both spring/neap and semi-diurnal cycle variations, meant that data could be extrapolated for a period of as much as a year [43-45].

c. Practical model

SHOM gathers, records and distributes official information necessary for maritime navigation. In fact, it provides long time records data of tide motion and the tidal current for spring and neap for various locations in chart form. These values are given in hourly intervals starting at 6 hours afore high waters and ending 6 hours later. The tide coefficients are used to derive a simple and practical model for tidal current velocities V . This service propose the following formula to determine the current velocity [11,46] :

$$V_{tide} = V_{nt} + \frac{(C-45)(V_{st}-V_{nt})}{(95-45)} \quad (10)$$

Where C is the tide coefficient which characterizes each tidal cycle (95 and 45 are respectively the spring and neap tide's average coefficients). V_{st} and V_{nt} are respectively the spring and neap tide current velocities for hourly intervals starting at 6 hours afore high waters and ending 6 hours later.

This practical model is unsophisticated, it needs only some interval current speeds and tide coefficients that can be gained from observations carried out by SHOM [47].

2.3. Kinetic energy extraction

Having presented the different model to calculate the tidal current, it is time to determine how much energy might be expected from a MCT in various tidal regimes. The total kinetic power extracted by a MCT can be calculated in a similar way of a wind turbine and it is expressed by the following equation [48]:

$$P_{hyd} = \frac{1}{2} \rho A V_{tide}^3 \quad (11)$$

This power depends on the water density ρ , on surface (A) swept by the marine propeller, and on the speed of the fluid V_{tide}^3 , thus the power of the resource increases very quickly with the current velocity, and it is considered that the hydrolien becomes interesting if the current exceeds 1.5 m/s. However only part of this power is recoverable and its turbine is modeled by the law of C_p (reactivity power coefficient) which transforms its capacity to extract the power from the marine currents [49].

$$P_m = \frac{1}{2} \rho A C_p V_{tide}^3 \quad (12)$$

The coefficient C_p depends on the turbine type, the number of blades and the tip speed ratio noted λ . The latter is the ratio between the velocity of the tip of the blade and the fluid velocity:

$$\lambda = \frac{\Omega R}{V_{tide}} \quad (13)$$

Where: Ω (rad/s) is the turbine rotation speed, R (m) is the diameter of the turbine and v (m / s) is the current speed.

The relations (12) and (13) will allow us to establish a set of characteristics determining the available power as a function of the turbine rotation speed for different water current.

3. Turbines concept, Installation and relative projects

Before any new concept is investigated, it is necessary to perform a preliminary study of the parameters that should be taken into account in the design process, for instance the velocity of the currents, the thrust forces, the depth of water, the nature of the seabed, the distance from the coasts and the specificity of the marine environment linked to weather conditions such as the salinity of the water, the site population and the wave regime [50,51]. All these parameters make it possible to select the bearing structure and the type of turbine. The flowchart in figure 3 and the figure 4 illustrate the different available MCT models and their classification:

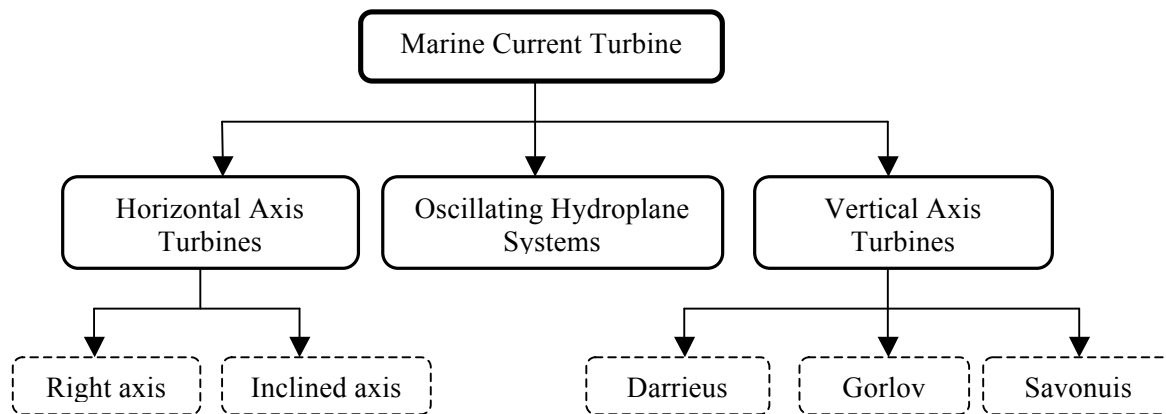


Figure 3: Classification of MCT

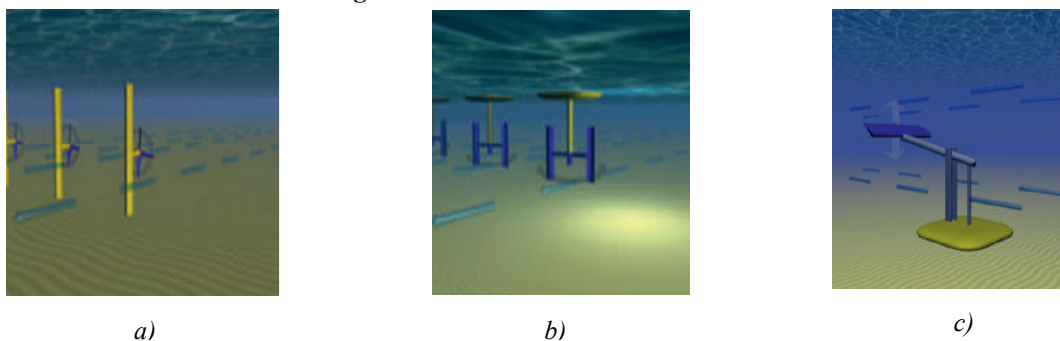


Figure 4 : a) Horizontal Axis Turbines,
b) Vertical Axis Turbines,
c) Oscillating Hydroplane Systems [52].

3.1. Horizontal axis turbines

Nowadays, the majority of the marine current devices are the horizontal axis turbines, because it is the direct adaptation of the well-established horizontal wind turbines to an aquatic environment [53]. For this MCT technology, the rotor's rotation axis is parallel to the incoming flow and the rotation is driven by the lift forces on the blades (figure 6. a) [54]. The turbine must be facing the flow to achieve optimum efficiency and therefore requires an orientation system to be positioned optimally when the direction of the tidal current changes. Depending on turbine design, the blades can either have a fixed pitch or variable pitch to enable the turbine to operate in inversed direction of the flow. A generator directly recovers the torque provided by the rotor shaft. There were many projects and concepts proposed and tested for horizontal axis system. In the table 2 below an overview of the main projects is given.

3.2. Vertical axis turbines

For vertical axis turbines, the rotation axis of the rotor is perpendicular to the incoming flow as shown in figure 5 [63]. One of the advantages of cross flow turbines is the insensitivity to the direction of the flow, the way that doesn't force the turbine to change its direction subsequently to the flow and the possibility of stacking several turbines on the same rotation shaft with the same generator. Similarly to horizontal axis turbines, the rotational speed is controlled according to the speed of the incoming current to maximize performance. The design of vertical axis turbine varies more than the horizontal axis turbine, including Savonius, Darrieus and H-rotor models (figure 5) [64]. Most of these designs have been successfully applied to the wind power industry. They extract energy from the tides in a similar manner to the horizontal axis turbines; however, the turbine is mounted such that its rotation axis remains vertical. It can convert the mechanical torque of the water surface directly without the complex transmission systems or a submerged nacelle. The major problems associated with the vertical axis turbines are high torque fluctuations with each revolution and no self-starting capabilities [65]. The technology of vertical axis turbines has been constructed and tested for their feasibility in commercial applications. Some projects based on these three types will be summarized in table 3.

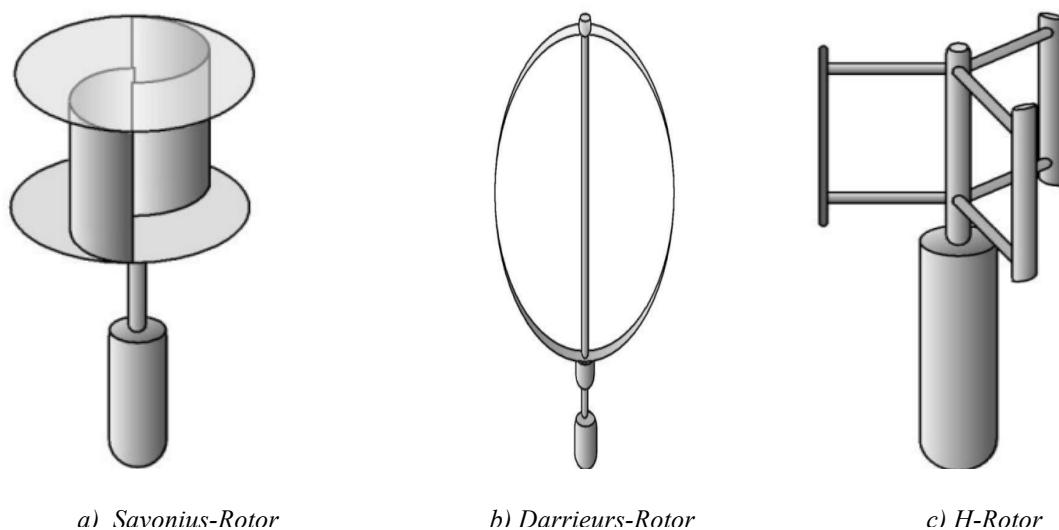


Figure 5: Three different types of vertical axis turbines[65].

3.2. Oscillating hydrofoil

In this technological concept, the MCT mimics the tail movement of marine mammals (figure 6. c) because of the lift forces exerted on the blade [72]. The leading edge of a submerged blade is arranged down current such that when the large hydroplane blade moves up and down or moves left and right, depending on the concept (whale tail or shark tail), the lift forces induce tangential force applied to the bearing arm. The angle of attack of the blade is adjusted in such a way that the lift force is maximal and the blade remains in the same direction of the incoming flow. The oscillating motion is subsequently dampened via hydraulic cylinders that will compress oil and store it in a high pressure tank. The high pressure oil will actuate a hydraulic turbine that drives a variable-speed electric generator [73]. The angle of attack of the blades requires continuous optimization during oscillations to maximize energy recovery. The table below presents the different projects of this technology.

Table 2 :Description and classification of horizontal axis technology used in MCT projects.

Builder	Power (MW)	Diameter Out (m)	Height (m)	Weight (Tonne)	Return of the experience	Illustration
Andritz (Hammerfest Strom)	1	23	30	300	Prototype of 0.3 MW tested in Norway (2003 to 2009) Prototype of 1 MW tested at the EMEC (2011/2012) [55].	
Sabella (D03, D10, D15)	0.2 à 2	3 à 15	5.5(D03) à 16 (D10)	290 (D10)	Prototype D03 tested in the estuary of Bénodet (2008/2009). Demonstrator project in the Fromveur [56].	
Voith Siemens (HyTide)	1	16	30	200	Prototype of 0.1 MW tested in Korea (2007). Prototype of 2 MW tested at the EMEC (since 2011). Pilot park project in the Raz Blanchard (2015) [57].	
Openhydro	0.5 à 2	6 à 16	21	850	Prototype OT6 tested at the EMEC (2008). Prototype OT10 tested in the Bay of Fundy (2009). Prototype OT16 (0.5 MW) tested at Bréhat (2011). Pilot park project in the Raz Blanchard (2015) [58] [59].	
SeaGen/Siemens	1.2	2*16	21	300	Seaflow prototype of 0.3 MW tested off Bristol (2003/2009). Prototype SeaGen tested in Northern Ireland (since 2008). Prototype tested in New York (2002-2006). Installation of 6 turbines connected to the grid (2008-2012) [60] [61] .	
Atlantis Ressources (AK 1000)	1	18	22.5	1300	Prototype HS 1000 of 0.5 MW tested at the EMEC (2010) [62].	

Table 3 : Description and classification of vertical axis technology used in MCT projects.

Builder	Power (MW)	Diameter Out (m)	Return of the experience	Illustration
Ponte diArchimède (Kobold turbine)	0.03 à 0.05	5	Test of a prototype of 0.07 MW in China (since 2006) [66][67].	
Gorlov Helical Turbine	1	1	The turbine in Maine, developed by ORPC (Ocean Renewable Power Company), USA, in 2012, is so called OCGen Turbine Generator Unit. It has a rated capacity of 150 kW [67][68].	
MCT Searius	1.3	-	The Searius project, which was submitted on May 16th to the Ademe AMI for the development of hydroelectric farms at the sites of Fromveur (Brittany) and Raz Blanchard (Basse-Normandie) A pilot plant of 10 hydro-turbines with a total capacity of 13 MW[69].	
Savonius-Rotorv	-	-	According to our literature, there are not many organizations who research the Savonius-type turbine for marine current energy except the Department of Marine Technology,Universiti Teknologi Malaysia [70][71].	

Table 4: Description and classification of Oscillating Hydroplane technology.

Builder	Power (MW)	Diameter Out (m)	Return of the experience	Illustration
Stingray turbine (UK)	0.15	-	It produced 250 kW at peak capacity and averaged 90 kW in a 1.5 m/sec measured current during its initial power cycles (Fig. I 23b). In 2005, this project was put on hold[74].	
bioSTREAM in Australia (BioPOWER)	0.2, 0.5, 1	-	It is based on the Thunniform-mode swimming propulsion of some swimming species, such shark, tuna, and mackerel. Due to the single point of rotation, this device can align with the flow in any direction, and can assume a streamlined configuration to avoid excess loading in extreme conditions. Systems are being developed for 500 W, 1 and 2 MW capacities to match conditions in various locations [75].	

4. Production of electricity and Direct Drive Generator Systems for Grid Connected Marines Current Turbine

4.1. Marine current generator model

Two types of electrical machines are generally used in the MCT industry for generation of electrical energy. These converters are Doubly-Fed Induction Generator (DFIG) and permanent Magnet Synchronous Generator (PMSG) [11][76] [77]. It should be noted that these electrical machines are the most used in the production of wind energy [78][79][80]. For a given application, the type of generator is chosen according to technical and economic factors (presence or not of the gearbox, variable speed, generation of high powers, mode of coupling to the electrical grid, etc.). The use of these two types of generators offers the possibility of direct or indirect connection to the electrical grid.

a. Doubly-Fed Induction Generator

The DFIG with wounded rotor presents a considerable advantage in the generation of high electric power [81]. The stator of this machine contains a three-phase winding which is directly connected to the grid and the three-phase winding of the rotor is connected to this same grid via a controlled converter [82][83]. The rectifier (machine side) operates at variable frequency with a low power of about 25% of the nominal power supplied to the grid. The inverter (grid side) adapts the output frequency of the system to that of the network which is 50 Hz. This configuration makes it possible to operate at variable speed in a range up to 30% around the synchronous speed [84]. The major disadvantage of this machine is the compulsory presence of the speed multiplier in the conversion chain. In addition, its conversion efficiency is lower than that of synchronous machines. The main components of this conversion system are illustrated in figure 6.

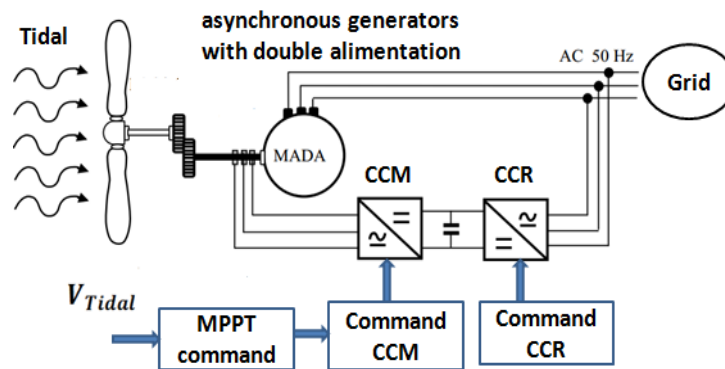


Figure 6: The connection of a tidal turbine system to the power grid via a DFIG.

b. Permanent Magnet Synchronous Generator

The PMSG is widely used in MCT applications, in particular because of its good conversion efficiency (close to 99%) compared to the asynchronous machine. It also allows variable speed operation provided that a power electronics interface is placed between its stator and the grid [85][86]. If this machine has a large number of pole pairs, it can be directly driven by the turbine, thus eliminating the gearbox which is a source of power losses. The excitation of this machine is ensured by permanent magnets and since it is driven by the turbine no input is available for regulating its voltage and its frequency, and for its connection to the electrical grid a power electronics interface is compulsory. The figure below illustrates the conversion chain of MCT system connected to the power grid and that uses PMSG [87][88].

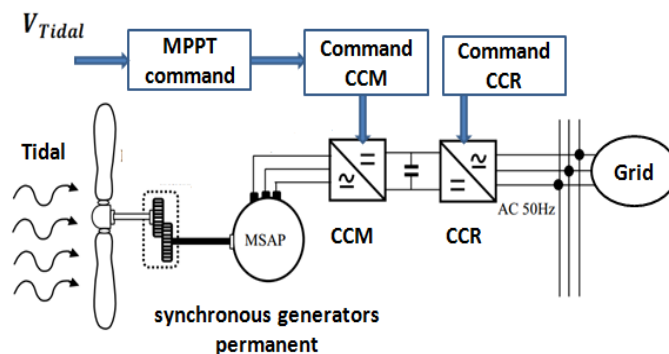


Figure 7: The connection of a tidal turbine system to the power via PMSG.

In marine applications and more particularly for MCT, the PMSG are more advantageous than asynchronous [89][90]. Moreover, The coupling of the PMSG to the grid requires the use of controlled converters (rectifier, inverter). The control strategies of the MCT are based on the variation of the mechanical power characteristics as a function of the speed of the tidal current, and the electrical power as a function of rotation speed [91] . At the machine side, the case of low and high sea current speeds are analyzed, evaluated and compared. When the speed of the tidal current is less than a nominal speed, the strategy known as Maximum Power Point Tracking (MPPT) is used. It consists in controlling the torque in order to regulate the number of generator revolutions. When the speed of tidal currents is greater than the nominal value, the mode of MPPT is changed into power limitation mode [92][93]. The grid is regulated so as to maintain the DC voltage constant and a unit power-factor.

4.2. Analysis of coupling possibilities of a direct-drive generator and a marines current turbine

The coupling of the turbine rotor with conventional generators with low number of poles (4 or 6) requires to increase the rotational speed of the rotor's shaft to meet the generator speed (which means a rise of rotational speed from less than 50 rpm on the turbine side to more than 1000 rpm on the generator side). By doing so, the torque transmitted to the generator is consequently reduced. In fact, to obtain an efficient electromechanical conversion, a gearbox is used. The gearbox may have several stages which can be a major source of failures and maintenance. Such a component increases the maintenance and the mass of the drive chain and lowers the overall efficiency of the system. for instance a 3-stage gearbox having a conversion ratio of several tens has an efficiency of the order of 90%. Furthermore, the MCT technology tendency questing for reliable and discrete solutions made it that more investigations are focused on direct drive. Thus, according to, the elimination of gearbox allows a quieter operation, reduced maintenance and increased availability.

In a direct-drive direct coupling, the generator is connected directly to the turbine without the use of gearbox, so that it rotates at the same speed as the turbine. The generator is driven at low speed and must produce high torque to produce the required power. Direct-drive generators generally have a large diameter and a big number of poles (about 100 poles for high-power generators), which makes it possible to minimize the mass and the cost of the generator. At equal diameter and power, the cost of the generator and its mass are higher than conventional generators. However, considering the entire drive chain, gearbox less solution offers increased reliability and reduced maintenance requirements. In the case of hydro-turbines, it is possible to couple the turbine and the direct-drive generator in two modes, 'Rim-Driven' and 'POD'[93][94].

a. Turbine / generator coupling in POD

In this case the generator and the turbine shafts are directly connected. Figure 8.a shows a generator coupled to the shaft of a wind turbine. The generator is placed in the nacelle behind the turbine rotor. In Figure 8.b a MCT that uses a direct-drive concept with 'POD' coupling is presented (Voith Hydro's 1MW Hytide). One of the important advantages of the POD coupling is that the shaft line is reduced which allows optimization of the shape of the hull and a better positioning of the rotor and thus improves the hydrodynamic efficiency of the turbine. In addition, the acoustic and vibratory level is improved by eliminating gearbox noise and vibrations and also by optimal positioning of the rotor up to the flow [95].

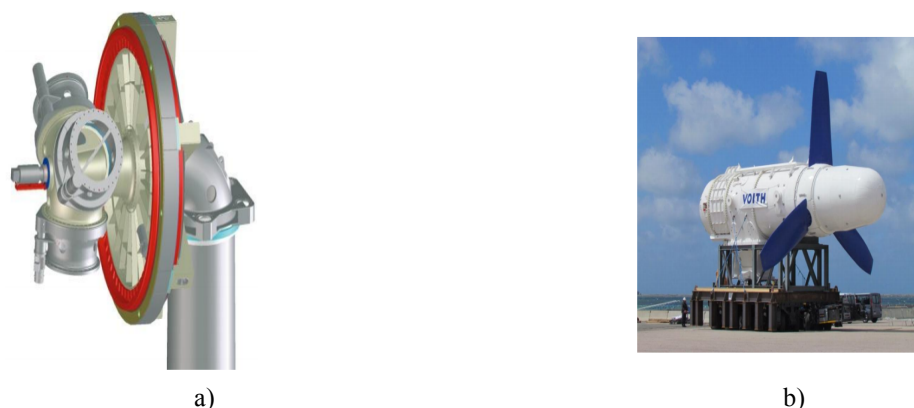


Figure 8: a) Wind direct-drive system E48 © Enercon, b) Hytide MCT of Voith Hydr.

Nevertheless one of the main difficulties at the design stage lies in choosing the optimum diameter of the machine. The torque is indeed proportional to the length times the diameter squared: a short machine of a large diameter is therefore relevant because it allows to optimize the quantity of materials. Moreover, a machine of great length is not very conceivable from the point of view of hydrodynamics. In contrast, an exaggerated diameter degrades the hydrodynamic efficiency of the turbine, which makes a better turbine diameter / rotor diameter ratio [95].

As we have seen, the electric generator is more and more close to the rotor. Thus, starting from the above POD electrical solution, it may be pertinent to imagine a new architecture of the electrical part that is voluminous and tends to reduce the hydrodynamic performances of the turbine. As we know, it is preferable to increase the radius of an electrical machine if it is desired to be compact while maintaining an advantageous level of electromagnetic losses. It therefore seems pertinent to seek to move the active parts of the machine from the rear of the rotor towards its periphery and then integrate them into the nozzle. This turbine concept is said to have circumferential drive, or Rim Driven [95].

b. Turbine / generator coupling in Rim-Driven

For a 'Rim-Driven' system with circumferential drive, the electric generator is directly driven and placed on the periphery of the rotor. The active parts of the rotor of the machine are in this technology attached to the periphery of the blades. The electrical generator is therefore directly driven by a rim located on the periphery of the turbine (Figure 9.a and Figure 9.b). This type of turbines can concern the naval propulsion (the electric machine then works as a motor) or the generation of tidal energy (in this case we speak of Rim-Driven generators). The concept was invented in the 1940s in Germany. Subsequently several patents were deposited between 1940 and 1970 on propellers driven by their circumference by either mechanical (gears) or electrical (electrical machines). Until 1980, patents filed mainly concerned the integration of asynchronous machines into Rim Driven. However, no significant experimental or commercial experiment was carried out during this period. Since the 1980s and especially the years 2000, several realizations and research based on the Rim-Driven principle have been carried out. From 2005, several commercial propulsion systems based on Rim-Driven technology have been developed. Following the example of the Rolls-Royce company which has developed a bow thruster, called 'Rim Thruster', with a power of 800 kW[96][97].

The Van der Velden (Netherlands) and Voith (Germany) companies also sell Rim-Driven bow thrusters with a capacity of around 100 kW. In addition to these industrial developments, academic research has investigated the Rim-Driven systems in recent years. In 2006, research work was carried out at the University of Southampton, United Kingdom, where iron-stator magnet machines were studied for Rim-Driven technology. More recent academic research has been conducted, as at the University of Manchester, UK, where a prototype of a 30kW permanent magnet electrical machine was produced in 2011 (Figure 9.c). At the level of hydroelectric applications, the most important achievement in Rim-Driven is currently the OpenHydro hydroelectric, of which two 500kW machines (Figure 10.a) are in the testing phase. This turbine was Installed and tested by EDF between 2012 and 2013 in Paimpol Bréhat, France. The research institute of the Naval School (RINS) has also developed a Rim-Driven prototype of low-power hydro-turbine to be tested in a basin (Figure 10.b)[95][96].

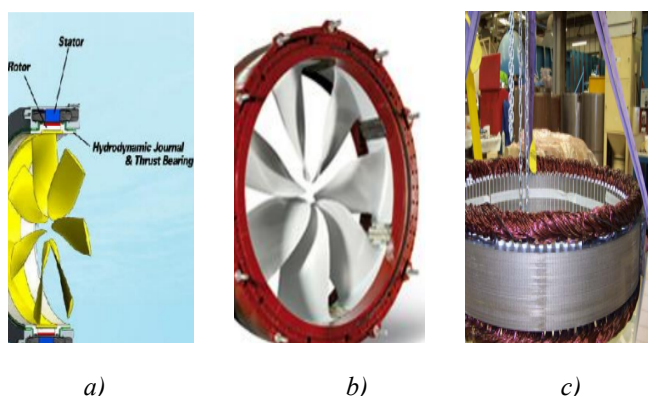


Figure 9: a) Arrangement of the electrical machine on the periphery of the propeller of a propellant Bow,
 b) Voith Hydro Rim-Driven bow thruster,
 c) Permanent magnet machine for a Rim-Driven thruster (30 kW).

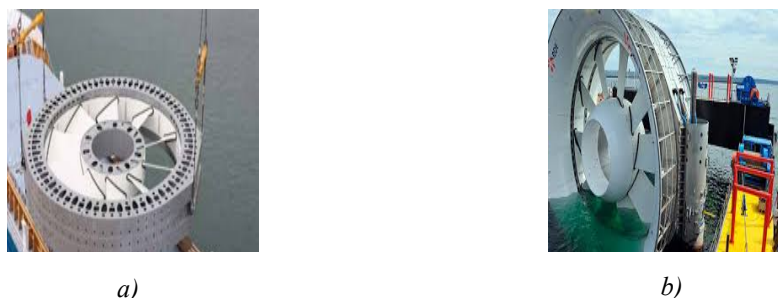


Fig. 10: a) View of the OpenHydro hydro-turbine rotor (500kW),
b) Demonstrator MCT in Rim-Driven RINS .

Compared to the more conventional 'POD' systems, advocates of Rim-Driven technology put forward a lower risk of cavitation and better hydrodynamic efficiency. Rim-Driven systems also have a larger generator compactness and more favorable thermal behavior because the water is on both sides of the electrical machine.

Conclusion

In this paper a review of technological state of art of marine tidal turbines generating electric energy has been carried out. Several important points were undertaken such as resource modeling, MCT types, MCT generators state of art and turbine and generator coupling.

Before installing a MCT, it is necessary to study precisely the resources of the considered site. For that, it is necessary to know the physical phenomenon of the tides which introduces the currents of tide and to know the calculated models of speed of these currents.

The choice and classification of turbine technologies used in MCT projects. Here the turbines were grouped according to several criteria such as: the axis of rotation of the turbine with respect to the flow direction of the fluid, the nature of the motion of the turbine (rotary or oscillating) and the technology of the blades.

A synthesis of the most advanced projects in terms of development is given. It shows some similarities with the conversion principles used in wind turbines. Indeed, the majority of the projects take up some of the concepts currently used for wind power. However, the specific nature of the turbine environment has led developers to rethink certain concepts and adapt them to the particular specifications of the hydro-turbines in order to find the best compromise between reliability (operating cost) and the cost of hydro Production and installation).

A comparative review of direct drive technologies (POD or Rim-driven) displayed that the both technologies had reached good maturity in the field of marine energies. They are developed for small or medium power turbines whose characteristics (diameter, speed, power) are close to those of high power propulsion. This concept has been studied and implemented for many years because unlike propellers, their sizes are less constraining and for these turbines the DFIG and PMSG machines can be envisaged.

References

1. F.O. Rourke, F. Boyle, A. Reynolds , *Appl. Energy*. 10 (2010) 398-409.
2. J. Ptasznik, *World Energy Assessment*. (2000).
3. I. Dincer, *Energy and environmental impacts: present and future perspectives Energy Sources, Part A*, (1998) 427–53.
4. S. A. Manne, G. Richels, *Efficiency and Equity of Climate Change Policy, Part 1*.(2000) 43-61.
5. M. Freedman, B. Jaggi, *Int. J. Account*. 40 (2005) 215–232.
6. S. Bilgen ,K. Kaygusuz, A.Sari , *Energy Sources*. 26 (12) (2004)1119–29.
7. I. Kralova, J. Sjöblom, *J. Dis Sci. Technol*. 31(3) (2010) 409–25.
8. N. L. Panwar, S. C. Kaushik, and S. Kothari, *Renew. Sustain. Energy Rev*.15 (2011) 1513–1524.
9. J. Griffiths, *International Development, Climate and Renewable Energy priorities, Scoping Dialogue on Sustainable Woody Biomass for Energy*. (2016) 21-22.
10. E. Sevigne, M. Carles, F. Brun, L. Rovira, J. M. Pagès, F. Camps, J. Rieradevall, X. Gabarrell, *Renew. Sustain. Energy Rev*. 15 (2011) 1133–1140.
11. H. CHEN, *Ph.D thesis*. France 11 Juillet 2014.
12. K. Bilen, O. Ozyurt, K. Bakırcı, S. Karsl, S. Erdogan, M. Yılmaz, O. Comaklı, *Renew. Sustain. Energy Rev*. (2008) 1529–1561.

13. D. Ahuja and M. Tatsutani, *Environ. Soc.* 2 (2009).
14. R. Pelc, and R. M. Fujita, *Mar. Pol.* 26 A247 (2002) 471 – 47.
15. S. Benelghali, M. Benbouzid, J.F. Charpentier, *IEEE IEMDC'07.*(2007) 1407-1412.
16. S. Benelghali, R. Balme, M. Benbouzid, J.F. Charpentier and F. Hauville, *IEEE J. Ocean. Eng.* 32 (2007) 786-797.
17. Z. Zhou, F. Sculler, J. Fr, Z. Zhou, F. Sculler, and J. Frédéric, *Renew. Sustain. Energy Rev.* (2013) 390-400.
18. O. Rourke, F. Boyle, *Renewable energy resources and technologies applicable to Ireland*, 13 (2009) 1975–1984.
19. S. Sheth, M. Shahideh, *IEEE* (2005).
20. J. M. B. Ilzarbe and J. A. Teixeira, *Recent Pat. Eng.* (2009) 178-193.
21. E. Lalander, *Renew. Sustain. Energy Rev.* 13 (2009) 1898-1909.
22. G. Hagerman and B. Polagye, *Methodology for Estimating Tidal Current Energy Resources and Power Production by Tidal In-Stream Energy Conversion (TISEC) Devices*, Report : EPRI – TP – 001 NA Rev 2, (2006).
23. I.G. Bryden, S.J. Couch, A. Owen, G. Melville, *Power Energy.* (Mar. 2007) 125–135.
24. Y. S. Lim, S. L. Koh, *Renew. Energy.* (2010) 1024–1032.
25. B. Polagye and M. Previsic, *System Level Design, Performance, Cost and Economic Assessment – Tacoma Narrows Washington Tidal In-Stream Power Plant*, Report: EPRI – TP – 006 WA. (2006).
26. R. Ahmadian, R. Falconer, B. Bockelmann-Evans, *Renew. Energy.* (2012) 107–116.
27. F. Behrouzi, A. Maimun, and M. Nakisa, *Int. J. Mec. Aeros. Indus. Mecha. Manuf. Eng.* (2014).
28. J.A. Clarke G. Connor, A. D. Grant, and C. M. Johnstone, *Renew. Energy.* (2006) 173-180.
29. S.M. Abu Sharkh, *Proceedings of IEE PEMD'02.* (2002) 486-491.
30. <https://earthsciencenhs.wikispaces.com/Tides> (Last accessed May 2014).
31. <http://www.oc.nps.edu/nom/day1/partc.html> (Last accessed May 2014).
32. <http://www.oc.nps.edu/nom/day1/partc.html> (Last accessed May 2014).
33. S. Draper, A. Thomas, A. Adcock, *Renew. Energy.* (2014) 650-657.
34. A. C. Baker, *The development of functions relating cost and performance of tidal power schemes and their application to small-scale sites*, in *Tidal Power*. London (1986).
35. “Tidal Analysis”, *Virginia Institute of Marine Science*, Available at web.vims.edu/physical/research/TCTutorial/tideanalysis.htm.
36. F. Lecornu, J. Paillet, H. Ravenel, *Coastal Operational Oceanography – Brest*. 13 14 (2008).
37. B. S. Love, *Ph. D thesis*. Scotland (2005).
38. M. B. Anwar, M. S. El Moursi, W. Xiao, *RPG Conference*. 22 December (2014).
39. Siemens SWT-6.0-154 6MW, Technical Report. available at http://www.swe.siemens.com/spain/web/es/energy/energias_renovables/eolica/Documents/6MW_direct_drive_offshore_wind_turbine.pdf (last accessed: December 2013).
40. P.L. Fraenkel, *Power and Energy.* 216 (2001).
41. S.M.R. Tousif, S.M.B. Taslim, *Int. J. Sci. Eng. Res.* (2011).
42. P.L. Fraenkel, *Power and Energy*, DOI: 10.1243/09576509JPE307, (2006).
43. M.K. Draško, and M. P. Čalasan, *Int. J. Eng Res. Tech (IJERT)* (2013).
44. A. Maheri, S. Noroozi, C. Toomer, and J. Vinney, *EWEC* (2006).
45. R.F. Nicholls-Lee, S.R. Turnock, S.W. Boyd, *2nd ICOE*, 15th – 17th October (2008).
46. S. Benelghali, *Ph.D thesis*, Université de Bretagne Occidentale (2009).
47. www.shom.fr/ (Last accessed May 2014).
48. M.C. Chainoux and R. H. Charlier, *Renew. Sustain. Energy Rev.* (2008) 2515–2524.
49. S. Benelghali, R. Balme, K. Le Saux, M.E.H. Benbouzid, J.F. Charpentier and F. Hauville, *IEEE J. Ocean. Eng.* (2007) 786-797.
50. Z. Zhou, M.E.H. Benbouzid, J.F. Charpentier, F. Sculler and T. Tang, *Renew. Sustain. Energy Rev.* (2013) 390-400.
51. M.J. Khan, G. Bhuyan, M.T. Iqbal and J.E. Quicoe, *Appl. Energy.* 1823-1835 (2009).
52. <http://www.emec.org.uk/marine-energy/tidal-devices/>
53. A. S. Bahaj, L. E. Myers, M. D. Thomson, and N. Jorge, *Seventh European Wave and Tidal Energy Conference*. Porto Portugal (2007).
54. R. Gaamouche, A. El Hasnaoui, A. Redouane, B. Belhorma, *IEEE Proce IRSEC*. Marrakech, Morocco (2016).
55. <http://www.andritzhydrohammerfest.co.uk/>

56. <http://www.sabella.fr/fiche.php?id=1>
57. <https://www.energiesdelamer.eu/publications/420-16voith-1-hydrolienne-hytide-1000-16-sort-du-chantier-naval-cmn>
58. B. Polagye, B.V. Cleve, A. Copping, and K. Kirkendall, *Scientific Workshop University of Washington*. Washington, USA, (2010).
59. I. Marbek, *Jupiter Hydro Inc*, March (2011).
60. Y. Li , H. K. Florig, *OCEANS*. (2006) 1-6.
61. <http://www.power-technology.com/projects/aktidalturbine/>
62. K. Tushar, A. Ghosh Mark . *Energy Resources and Systems, Volume 2: Renewable Resources, Springer Dordrecht Heidelberg*. London New York (2011) .
63. F. O. Rourke, F. Boyle, A. Reynolds, *Renew. Sustain. Energy Rev.*14 (2010) 1026-1036.
64. J. Joslin, E. Celkis, C. Roper, *IEEE Proce oceans*, San Diago (2013).
65. A. Moroso, *Tidal Energy Summit*. london 28 (2007).
66. <http://www.seapowerscrl.com/ocean-and-river-system/kobold>
67. A. L. Niblick, *Ph.D thesis*. University of Washington, 2012.
68. <http://www.gcktechnology.com/GCK/pg2.html>
69. O. Yaakob, Y. Ahmed, M. Mazlan, K. Jaafar, R. Muda, *World Appl. Sc. J.* 26 (2013) 91-98.
70. B. Yaakob, K. B. Tawi, and D. T. S. Sunanto, *IJE Transactions A: Basics*, 23 (2010) 81-87.
71. J. BOSSARD, *Ph.D thesis*, Université de Grenoble (2012).
72. P. Campagna, *Ph.D thesis*. Québec, Canada (2013).
73. M.E.H. Benbouzid, *Proceedings of ICEM'06*, Chania (Greece), (2006).
74. http://www.esru.strath.ac.uk/EandE/Web_sites/09-10/MCT/html/Home
75. S.E. Ben Elghali , *JCGE'08 LYON*, (2008).
76. S.E. Ben Elghali, M.E.H. Benbouzid, J.F. Charpentier, *XIX International Conference on Electrical Machines - ICEM* .Rome (2010).
77. F. Jeffali, B. EL Kihel, A. Nougououi, F. Delaunois , *J. Mater. Environ. Sci.* 6 (4) (2015) 1192-1199.
78. S.E. Ben Elghali, M.E.H. Benbouzid, J.F. Charpentier, *IEEE J. Ocean. Eng.* 37, (2012).
79. A. M. ANDREICA , *Ph.D thesis*, Laboratoire de Génie Electrique de Grenoble (2014).
80. A. Abdelli, *Ph.D thesis* .Institut national polytechnique de Toulouse (2007).
81. F. Poitier, *Ph.D thesis*. Université de Nantes (2003).
82. S. Benelghali, M. E. H. Benbouzid, and J. F. Charpentier, *IET Renewable Power Generat.*4 (2010)1–11.
83. Y. Lei, A. Mullane, G. Lightbody, and R. Yacamini, *IEEE Trans. Energy Conv.*21 (2006).
84. S. Mouty, *Ph.D thesis*, Université de Franche-Comt (2013).
85. Z. Zhou, F. Scuiller, Z. Zhou, F. Scuiller, *IEEE J. Ocean. Eng.* 40 (3) (2015) 536-545.
86. S. Benelghali, M. Benbouzid, and J. F. Charpentier, *Rev. Energie Renov.* 15 (2012) 29 – 41.
87. M. Andreica, S. Bacha, and D. R. J. Guiraud, *Rev. Energie Renov.* 11 (2008) 493 – 502 .
88. M. M. Elzalabani, F. H. Fahmy, A. E. A. Nafeh, and G. Allam, *TELKOMNIKA Indones. J. Electr. Eng.* 13(2015) 57-64.
89. O. Keysan, A. S. McDonald, and M. Mueller, *Proc. IEEE Int. Electr. Mach. Drives Conf. Niagara Falls*. Canada (2011) 224–229.
90. K. Yue, S. Ape lf röjd, M. Leijon, *J. Control Sc. Eng* . 2 (2013) 10 pages.
91. G. Mokryani, P. Siano, A. Piccolo, Z. Chen, *IEEE Sys.*(2012).
92. M. Andreica, S. Bacha, D. Roye, J. Guiraudkjh, *Rev. Energie Renov.* 11 (2008) 493 – 502.
93. E. Pelerin, P. Toulouse, F. Pilorge, *Congrès SHF (EMR)*. Brest 09-10 (2013).
94. L. DROUEN, *Ph.D thesis*, École Nationale Supérieure d'Arts et Métiers de Paris (2010).
95. L. Terme, N. Gérard, *Congrès SHF (EMR)*. Brest 09-10 (2013).
96. P. M. Tuohy, *Ph.D thesis*, University of Manchester (2011) .
97. D. Bang, H. Polinder, G. Shrestha, J.A. Ferreira, *European Wind Energy Conference*, (2008) 1-7.

(2018) ; <http://www.jmaterenvirosci.com>